

# Ligand-assisted J-type aggregates of zinc porphyrin: anticooperative molecular organization in self-assembled bolaamphiphile†

Mitsuhiro Morisue,\* Takefumi Morita and Yasuhisa Kuroda

Received 24th March 2010, Accepted 20th May 2010

First published as an Advance Article on the web 9th June 2010

DOI: 10.1039/c004636a

Bolaamphiphilic zinc porphyrins bearing a 2-pyridylethynyl or 4-methoxyphenylethynyl group, Zn(PyPor) or Zn(ArPor), respectively, were newly synthesized in order to explore the molecular organizing behaviours within the interior hydrophobic layer of aqueous self-assemblies. Well-ordered J-type aggregates of Zn(PyPor) were formed in aqueous self-assembled bolaamphiphile, whereas J-type aggregates of Zn(ArPor) were disordered. The titration experiments suggest that axial coordination bond improves the structural uniformity of the J-type aggregates of Zn(PyPor). In a homogeneous isotropic media, on the other hand, Zn(PyPor) formed an antiparallel dimer through self-complementary coordination. Unprecedented molecular organization of ligand-assisted J-type aggregates is described in the term of anticooperative effect under the bulk conditions.

## 1. Introduction

The formation of organized porphyrin assemblies through axial coordination has prompted significant efforts to construct sophisticated molecular architectures aiming at artificial photosynthesis and further novel photophysical applications.<sup>1</sup> Fundamentally, an association constant defines such dynamic structures as a function of the concentration.<sup>2</sup> The stationary dynamic structures are normally designed considering a homogeneous isotropic solution. The organized geometry of multiporphyrin assemblies is controllable by virtue of the rigid platform of porphyrin macrocycle.<sup>1</sup> Of particular importance, a cooperative effect stems from a preference of *intra*-complex interactions over *inter*-molecular interactions in isotropic solutions.<sup>2b</sup> In principle, if the contribution of solvent molecules is ruled out, a coordination bond should be formed regardless of the magnitude of binding constant, where a cooperative effect no longer remains. Then, dynamic structures should be altered into an unprecedented form under a bulk condition.

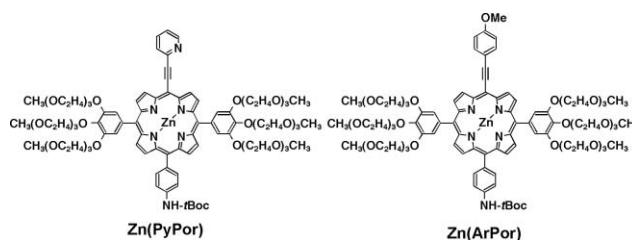
The ligand-appended porphyrinatozinc(II) is well known to exclusively form an antiparallel dimer *via* self-complementary coordination.<sup>1,3–6</sup> This is accomplished by the positively allosteric cooperativity possible by the intra-dimer coordination being much more favorable than the initial coordination in isotropic solutions. On the other hand, another possible staircase configuration can emerge as a slipped-stacked array, the so-called J-type aggregates, which has never been observed, otherwise than with a specific aid such as porphyrin–graphite surface interaction.<sup>5</sup> From the viewpoint of the structural and functional relevance to photosynthetic light-harvesting complex, the staircase porphyrin assemblies through electrostatic interaction have been the subject of intense research.<sup>7–9</sup> The present manuscript discloses an unusual formation of J-type aggregates of zinc porphyrins in a bulk condition employing the aqueous self-assemblies.

Amphiphilic assemblies incorporating porphyrin have been reported as successful models for the primary photosynthesis.<sup>10</sup> The self-assembled amphiphile partitions the interior hydrophobic layer from the outer solvent and provides a condensed phase fluid in aqueous solution.<sup>11</sup> Such a two-dimensional layer may be seen as analogous to a cuvette with nanometre-order optical path length. Herein, we describe the synthesis of nonionic bolaamphiphilic porphyrins and subsequent investigation of the bulk self-coordinating properties within the aqueous self-assembly.

## 2. Results and discussion

### 2.1. Molecular organization in aqueous self-assemblies

The present molecular design of Zn(PyPor) introduces nitrogenous-ligand aiming at pyridyl-to-zinc self-coordination,<sup>4,5</sup> and dendritic oligoether groups as nonionic hydrophilic side-chains to solubilize in the aqueous media (Scheme 1). The homologous non-coordinating porphyrin, Zn(ArPor), has been synthesized as a reference compound, as described in the Experimental section (*vide infra*, Scheme 2).

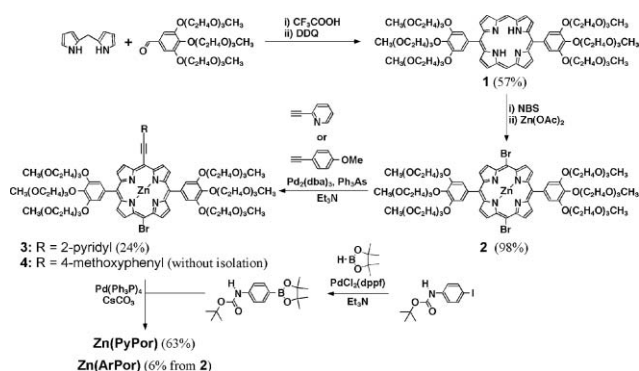


Scheme 1 Chemical structures of Zn(PyPor) and Zn(ArPor).

Aqueous self-assemblies of Zn(PyPor) were prepared by injection of a methanol solution of the porphyrin into distilled water followed by aging for a few days. A stationary Soret band emerged at 464 nm indicating considerable expansion of the  $\pi$ -system above that of the conventional antiparallel dimer (Fig. 1a). A remarkable bathochromic shift should be the outcome of formation of

Department of Biomolecular Engineering, Kyoto Institute of Technology, Matsugasaki, Sakyo-ku, Kyoto, 606-8585, Japan. E-mail: morisue@kit.ac.jp

† Electronic supplementary information (ESI) available: Syntheses, experimental observations in isotropic solutions, and preparation of aqueous self-assemblies. See DOI: 10.1039/c004636a



**Scheme 2** Synthetic routes of Zn(PyPor) and Zn(ArPor).

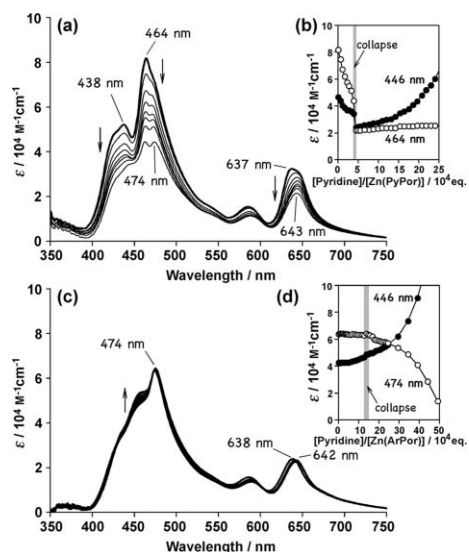


**Fig. 1** Spectral titration of Zn(PyPor) (a) and Zn(ArPor) (c) with pyridine in water at 25 °C, up to the collapse of the amphiphilic assemblies. Spectral change was recorded after successive additions of *ca.*  $5 \times 10^3$  equiv of pyridine. Plots of absorbance at the selected wavelengths (b and d).

J-type aggregates.<sup>7–9,12</sup> Such bathochromism was also observed for Zn(ArPor) in aqueous assemblies (Fig. 1c). The bulkiness of dendritic oligoether side group may be effective to preclude from H-type cofacial stacking and to form J-type aggregates.<sup>13</sup>

Epifluorescence microscopic observations identified fluorescent spheres elucidating that the bolaamphiphilic porphyrin was spontaneously assembled into spherical aggregates. The size of spherical assemblies was in the order of micrometres, being at least larger than 0.45  $\mu\text{m}$  judging from complete disappearance of the Soret band after passing the solution through membrane filter with a pore diameter of 0.45  $\mu\text{m}$ . Thus, J-type aggregates were formed within the aqueous self-assemblies.

Notably, the pyridyl group plays a crucial role in organization of the well-ordered J-type aggregates. The aqueous assemblies of Zn(PyPor) exhibited emission seventy times stronger than that of Zn(ArPor) (Fig. 2). In general, structural disorder dissipates excited singlet through an energy sink leading to weak fluorescence of the chromophore assemblies (Scheme 3d).<sup>14</sup> Therefore, it is clear that the pyridyl ligand significantly improves the structural uniformity of the J-type assemblies as compared to that obtained

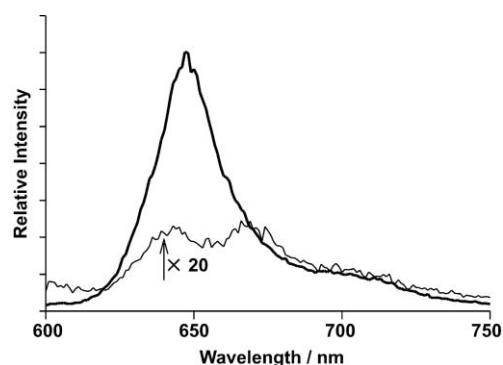
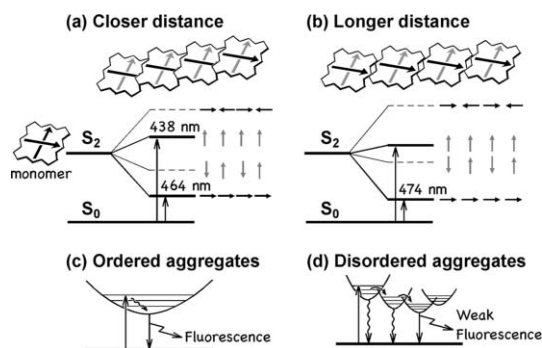


**Fig. 2** Emission spectra of the aqueous assemblies of Zn(PyPor) (thick line) and Zn(ArPor) (thin line, magnified by twenty times) observed by excitation at 580 nm.



**Scheme 3** Schematic energy diagrams of exciton coupling of J-type aggregates with closer distance (a) and longer distance (b). Solid lines denote optically allowed transitions and dotted lines are optically forbidden. Schematic illustration of fluorescent processes for ordered (c) and disordered aggregates (d).

through sole  $\pi$ - $\pi$  stacking. Highly ordered J-type aggregates are expected to be driven by pyridyl-to-zinc axial coordination.

As long as the aqueous self-assemblies remain, spectral properties should be apparently relevant to the bulk organized structure. To explore the bulk self-organization properties of Zn(PyPor), the effect of a nitrogenous ligand was then investigated in aqueous solution. Axial coordination of the external ligand should undergo a permeation process limited by a hydration–dehydration process as parameterized by the octanol/water partition coefficient,  $\log P$ , index.<sup>15–17</sup> Therefore, introduction of an external ligand should lead to diverse effects, *i.e.*, dilution of the concentration of porphyrin within the hydrophobic layer in aqueous self-assemblies and competitive axial coordination. Titration experiments on Zn(PyPor) showed a two-step discontinuous spectral change indicating structural transition within the aqueous self-assemblies followed by its collapse, coincident with changes in the morphology as observed by epifluorescence microscopy. In this way, the titrations with pyridine and 2,6-lutidine are performed up to the point of collapse in the following section.

Upon addition of pyridine as the competitive ligand, the bathochromic Soret band of Zn(PyPor) at 464 nm was duplicated to give another bathochromic band at 474 nm (Fig. 1a). At the same time, the shorter Soret band at 438 nm disappeared. Also bathochromism of the Q band was enhanced from 637 nm to 643 nm. The enhanced bathochromism suggests larger dislocation of interplane distance, based on Kasha's molecular exciton

theory (Scheme 3a and 3b).<sup>8b,12</sup> The observation of an increased bathochromic band was closely reminiscent of that observed for aqueous assemblies of Zn(ArPor), and is considered to originate from the intrinsic  $\pi$ -stacking properties of bolaamphiphilic porphyrin (Fig. 1c). On the other hand, the spectral titration of Zn(ArPor) assemblies were faint. These spectral changes were in sharp contrast to dissociation behavior, as emphasised in the plots of the bathochromic and monomeric Soret bands for the Zn(PyPor) assemblies showing biphasic change (Fig. 1b). On the other hand, those for the Zn(ArPor) assemblies were dissociated in a quasi-single phasic fashion (Fig. 1d). The susceptibility of Zn(PyPor) to coordination by an axial ligand suggests that self-coordination drives highly ordered J-type aggregates found in the aqueous self-assemblies.

Additionally, the titration experiments were conducted with an aqueous solution of 2,6-lutidine. Steric hindrance of the two methyl groups in this case significantly disturbs the coordination capacity of nitrogen atom of 2,6-lutidine, while the degree of permeation should be much higher than that of pyridine.<sup>15,16</sup> A dilution effect was observed for 2,6-lutidine in which the self-coordination of Zn(PyPor) was dissociated into smaller aggregates in the two-dimensional assemblies; here, monomeric species may be predominant judging from the absorption maxima at 444 nm (Fig. 3a). A dilution effect of 2,6-lutidine was also observed in disstacking the  $\pi$ - $\pi$  interaction of the Zn(ArPor) J-type aggregates (Fig. 3b). These observations are pertinent to the small binding constants for self-coordination of Zn(PyPor) in a homogeneous isotropic solution (*vide infra*).

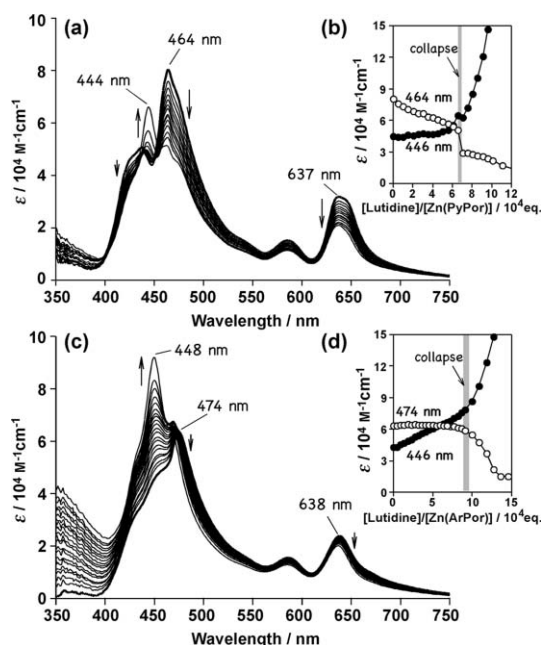


**Fig. 3** Spectral titration of Zn(PyPor) (a) and Zn(ArPor) (c) with 2,6-lutidine in water at 25 °C, up to the collapse of the amphiphilic assemblies. Spectral change was recorded after successive additions of *ca.*  $5 \times 10^3$  equiv of pyridine. Plots of absorbance at selected wavelengths (b and d).

Addition of external ligands was certainly effective in terms of both competitive coordination and dilution of the amphiphilic assemblies. The observations elucidates some parts of essential

principles underlying the bulk molecular organization, although the observations should involve plural thermodynamic factors in the strict sense. Further elucidation of the bulk molecular organization in the heterogeneous system is difficult. The self-organizing behaviours of Zn(PyPor) in isotropic organic media may be predictive of some aspects of the stacking properties in aqueous self-assemblies.

## 2.2. Self-complementary coordination in isotropic solutions

Zn(PyPor) showed self-organizing behaviour when using  $\text{CDCl}_3$  as a non-coordinating solvent in  $^1\text{H}$  NMR spectra. The protons of  $\beta$ -pyrrole and pyridyl residue showed upfield shift, suggesting ring-current shielding due to the close proximity to the mutual porphyrin plane (Fig. 4). Assuming the equilibrium between monomer and dimer, the concentration dependence of  $^1\text{H}$  NMR spectra indicated an association constant ( $K_1 \times K_2$ , in Scheme 4) of  $\sim 10^1 \text{ M}^{-1}$  based on the nonlinear least square fitting.<sup>†</sup> On the other hand, no organized behaviour was detected for Zn(PyPor) when using  $\text{CD}_3\text{OD}$  as a coordinating solvent. Further, Zn(ArPor) showed no concentration dependence in either of the solvents. Hence, the self-organization behaviour was a specific phenomena for Zn(PyPor) in a non-coordinating solvent under highly concentrated conditions. Self-organization is thus assignable to formation of an antiparallel dimer through self-complementary pyridyl-to-zinc coordination, according to a previous report.<sup>6</sup> The small binding constant for self-complementary coordination may be attributed to low coordination ability of 2-ethynylpyridyl group as follows.

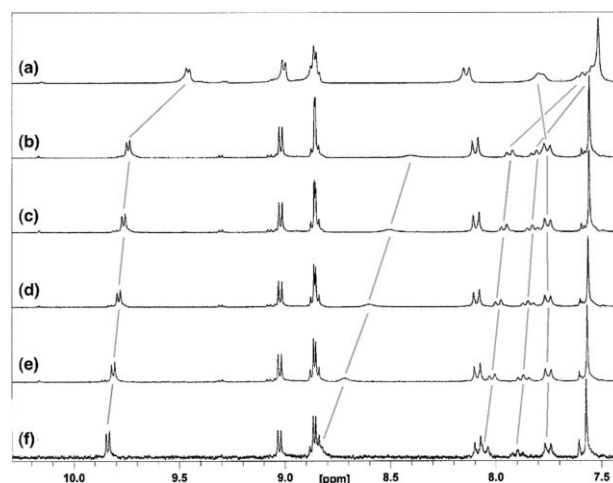
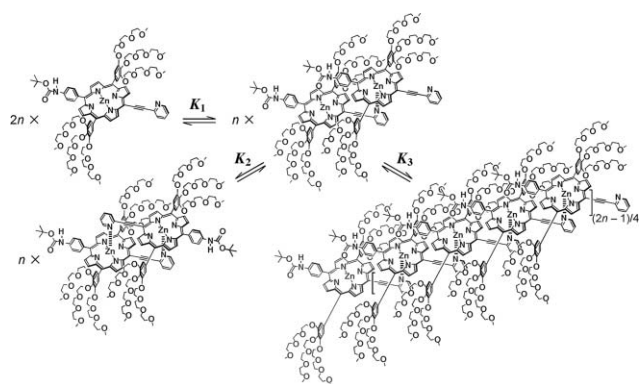


**Fig. 4** Representative  $^1\text{H}$  NMR spectra (300 MHz) of Zn(PyPor) at various concentrations in  $\text{CDCl}_3$ ;  $9.2 \times 10^{-2} \text{ M}$  (a),  $1.0 \times 10^{-2} \text{ M}$  (b),  $7.5 \times 10^{-3} \text{ M}$  (c),  $5.0 \times 10^{-3} \text{ M}$  (d),  $2.5 \times 10^{-3} \text{ M}$  (e), and  $5.0 \times 10^{-4} \text{ M}$  (f).

The initial binding constant  $K_1$  of the 2-ethynylpyridyl group to the zinc atom was estimated to be less than  $\sim 10^{-5} \text{ M}^{-1}$  from the titration experiment of 2-phenylethynylpyridine with Zn(PyPor) in chloroform.<sup>†</sup> This estimated value is too small to rationalize the self-organization behaviour observed in the  $^1\text{H}$  NMR. This fact proves formation of self-complementary coordination through a second binding constant  $K_2$  at least as large as  $10^6 \text{ M}^{-1}$  to account for the observed self-association constant of  $\sim 10^1 \text{ M}^{-1}$ . Such a dimensionless constant would be much more favourable





**Scheme 4** Possible coordination equilibria of Zn(PyPor). Binding constants;  $K_1$  for the single coordination to form a dimer,  $K_2$  for the second intradimer coordination to form an antiparallel dimer *via* self-complementary coordination, and  $K_3$  for successive coordination to form J-type aggregates.

than the initial binding process in fulfilling the prerequisite for positively allosteric cooperativity to exclusively form an antiparallel Zn(PyPor) dimer.<sup>2b</sup> The initial nucleation induced the second coordination bond through dimensionless binding equilibrium, leading to self-complementary coordination in  $\text{CDCl}_3$ . Eventually, self-organizing behaviours of Zn(PyPor) are consistent with the formation of a self-complementary dimer.

### 2.3. Anticooperative effect in a bulk medium embedded in self-assembled bolaamphiphile

Based on the above insights in homogeneous isotropic solutions, let us consider the properties of molecular organization in the aqueous self-assemblies. In isotropic solution, self-complementary coordination is inherent in ligand-appended zinc porphyrins, wherein a positively allosteric cooperative effect excludes the formation of J-type aggregates because of disadvantage in the entropy change. Thus, roles of the solvent must be key in the free energy change. Consequently, the initial nucleation promotes the second intra-complex association leading to self-complementary coordination (Fig. 5).

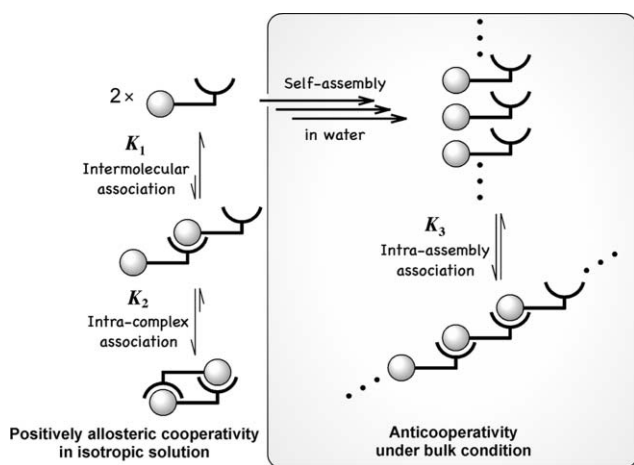


**Fig. 5** Schematic illustration of positively allosteric cooperative system in homogeneous isotropic solution and anticooperative system in the aqueous self-assemblies.

In aqueous media, on the other hand, the initial nucleation is achieved by the formation of the aqueous self-assemblies. Likewise the formation of the second coordination in an antiparallel dimer, the nucleation compensates the small coordination capacity. Moreover, the relative difference in the binding affinity should not remain in the bulk condition—the so-called anticooperative effect, wherein all the porphyrin constituents are equivalent. The possible binding processes obey the sole dimensionless equilibria assuming the single binding mode of the pyridyl-to-zinc coordination. To this end, the formation of successive coordination bond should be preferable to the self-complementary one in some probability (Fig. 5). Along the bulk equilibria, small activation barrier for dissociation of the antiparallel dimer may be proper for smooth production of the J-type aggregates, avoiding kinetic entrapment into the antiparallel dimer. Hence, Zn(PyPor) is likely to produce successive coordination bonds in a unique fluidic medium within the aqueous self-assemblies.

## 3. Conclusions

In summary, we have exploited a bulk molecular organization within the interior hydrophobic layer of the self-assembled bolaamphiphile. Comparable studies of molecular organizing behaviour drew contrasting results in terms of the thermodynamic equilibria between the assemblies in aqueous solution and those in isotropic organic solvent. Consequently, highly ordered J-type aggregates of Zn(PyPor) have been provided by the aid of self-coordination under the conditions where solvent molecule is ruled out. To the best of our knowledge, aqueous J-aggregates of porphyrin normally assemble through electrostatic interactions under acidic conditions.<sup>9,10</sup> On the other hand, the structure of the J-type aggregates of Zn(PyPor) was modulated by an external ligand under neutral conditions. Such ligand-directed structural tunability offers a great advantage in a functionalization of porphyrin J-type aggregates. We are convinced that the anticooperative molecular organization methodology opens the way to design elaborate polymeric architectures.

## 4. Experimental section

### 4.1. General procedures

NMR spectra were recorded on AV-300 (BRUKER). MALDI-TOF MS spectra were observed by using dithranol as the matrix by Autoflex II (BRUKER). Recycling gel-permeation chromatography (GPC) was carried out by LC-9101 (Japan Analytical Industry Co., Ltd.) connecting column of JAIGEL-3H and -2H with chloroform as the eluent. UV-visible and fluorescence spectra were recorded on the spectrophotometer (Multispec-1500, Shimadzu) and the fluorescence photospectrometer (F-4500, Hitachi), respectively.

### 4.2. Procedures of synthesis

All reagents were used as received otherwise described. Dehydrated solvents were prepared by general procedures; *N,N*-dimethylformamide (DMF) and triethylamine were distilled over calcium hydride under vacuum, tetrahydrofuran (THF) and 1,4-dioxane were distilled over sodium/benzophenone ketyl, toluene

was distilled over melting sodium.  $\text{Pd}_2(\text{dba})_3$  (dba = *trans,trans*-dibenzylidenacetone) was prepared by the general procedure; to the solution of palladium chloride (0.43 g, 1.8 mmol) and sodium acetate (0.40 g, 4.9 mmol) in methanol (15 mL) was added dba (0.17 g, 0.94 mmol) at 50 °C under argon atmosphere and then recrystallization of the precipitate obtained from chloroform.

**4.2.1. 5,15-Bis[3,4,5-tris(9-methoxy-1,4,7-trioxanonyl)phenyl]porphyrin (1).** The titled compound **1** was prepared by the modified literature method.<sup>18</sup> The solution of 3,4,5-tris(9-methoxy-1,4,7-trioxanonyl)benzaldehyde (0.86 g, 1.5 mmol) and dipyrromethane (0.22 g, 1.5 mmol) dissolved in chloroform (300 mL) was deaerated by bubbling with nitrogen gas for 5 min. The mixture was stirred with TFA (trifluoroacetic acid, 1.0  $\mu\text{L}$ , 13  $\mu\text{mol}$ ) at room temperature in the dark for 14 h. To the reaction mixture was added DDQ (2,3-dichloro-5,6-dicyano-1,4-benzoquinone, 0.33 g, 1.5 mmol) as the oxidant and stirred for additional 3.5 h. The reaction mixture was washed successively with aqueous saturated sodium hydrogencarbonate and brine. The organic layer separated was dried over anhydrous sodium sulfate. The crude material was subjected to the silica-gel chromatographic separation with chloroform–methanol (95/5 and 98/2, v/v) as the eluent. Porphyrin **1** was obtained as a viscous purple substance (0.59 g, 0.41 mmol; 57%). The compound was identified by  $^1\text{H}$  NMR and MALDI-TOF MS, which were identical with those in previous report.<sup>18</sup>

**4.2.2. 5,15-Bisbromo-10,20-bis[3,4,5-tris(9-methoxy-1,4,7-trioxanonyl)phenyl]porphyrinatozinc(II) (2).** To the solution of porphyrin **1** (0.69 g, 0.48 mmol) in chloroform (50 mL) was added NBS (*N*-bromosuccinimide, 0.18 g, 0.99 mmol) at –40 °C and stirred for 60 min. Bromination was quenched by addition of acetone (*ca.* 5 mL) and the solvent was removed under reduced pressure. The crude material redissolved in chloroform (50 mL) was treated with saturated zinc acetate in methanol (3 mL) at room temperature for 2 h. The reaction mixture was washed with aqueous saturated sodium hydrogencarbonate and brine. The organic layer separated was dried over anhydrous sodium sulfate. Purification by silica-gel column chromatography with chloroform–methanol (98/2, v/v) afforded dibrominated porphyrin **2** as a viscous brown substance (0.78 g, 0.47 mmol; 98%).  $^1\text{H}$  NMR (300 MHz,  $\text{CDCl}_3$ ):  $\delta$  = 2.35–4.05 (m, 78H; ethylene), 4.35 (t,  $J$  = 5.0 Hz, 8H; Ph-3,5- $\text{OCH}_2$ -), 4.50 (t,  $J$  = 4.9 Hz, 4H; Ph-4- $\text{OCH}_2$ -), 7.54 (s, 4H; Ph) 8.97 (d,  $J$  = 4.7 Hz, 4H; pyrrole- $\beta$ ), 9.68 (d,  $J$  = 4.7 Hz, 4H; pyrrole- $\beta$ ) ppm.  $^{13}\text{C}$  NMR (75 MHz,  $\text{CDCl}_3$ ):  $\delta$  = 58.34, 58.64, 68.84, 69.47, 69.78, 70.12, 70.24, 70.38, 71.17, 71.56, 72.30, 77.79, 104.76, 115.18, 121.57, 132.88, 133.31, 137.65, 137.73, 150.00, 150.32, 150.62 ppm. MALDI-TOF MS (dithranol):  $m/z$ : calcd for  $\text{C}_{74}\text{H}_{102}\text{Br}_2\text{N}_4\text{O}_{24}\text{Zn}$ : 1652.45; found: 1652.36.

**4.2.3. 5-Bromo-15-(2-pyridylethynyl)-10,20-bis[3,4,5-tris(9-methoxy-1,4,7-trioxanonyl)phenyl]porphyrinatozinc(II) (3).** The mixture of porphyrin **2** (0.66 g, 0.40 mmol) and 2-ethynylpyridine<sup>19</sup> (40 mg, 0.39 mmol) in THF (20 mL) with triethylamine (3.2 mL) was deoxygenated by freeze-pump-thaw cycles and purged with argon gas in a Schlenk flask. The mixture was added triphenylarsine (65 mg, 0.21 mmol) and  $\text{Pd}_2(\text{dba})_3$  (29 mg, 32  $\mu\text{mol}$ ), and then stirred at 50 °C in the dark for 24 h. The crude mixture was washed with brine. The organic layer separated was dehydrated by anhydrous sodium sulfate. Porphyrin

**3** was roughly purified by elution from a triethylamine-treated silica-gel column chromatography with chloroform–ethyl acetate–methanol (90/7/3, v/v/v) as a viscous green substance (103 mg, 0.095 mmol; 24%). This material was used for the next step without further purification. MALDI-TOF MS (dithranol):  $m/z$ : calcd for  $\text{C}_{81}\text{H}_{106}\text{BrN}_5\text{O}_{24}\text{Zn}$ : 1675.57; found: 1675.58.

**4.2.4. 5-{*N*-(*tert*-butoxycarbonyl)-4-anilino}-15-(2-pyridylethynyl)-10,20-bis[3,4,5-tris(9-methoxy-1,4,7-trioxanonyl)phenyl]porphyrinatozinc(II), Zn(PyPor).** The mixture of porphyrin **3** (0.12 g, 0.074 mmol) and pinacol {4-*N*-(*tert*-butoxycarbonyl)aminophenyl}boronate (30 mg, 0.094 mmol) in DMF (6 mL) and toluene (12 mL) was deoxygenated by freeze-pump-thaw cycles and flushed with argon gas in a Schlenk flask. The mixture was added caesium carbonate (26 mg, 81  $\mu\text{mol}$ ) and  $\text{Pd}(\text{PPh}_3)_4$  ( $\text{PPh}_3$  = triphenylphosphine) (12 mg, 9.8  $\mu\text{mol}$ ), and then allowed for stirring at 80 °C in the dark for 5 h. The reaction mixture was passed through Celite pad. After removal of the solvent, the crude material dissolved in dichloromethane was washed with water and brine. The titled material was purified by silica-gel column chromatography with chloroform–ethyl acetate–methanol (90/7/3, v/v/v). Further purification by recycling GPC with chloroform as the eluent afforded Zn(PyPor) as a viscous green substance (83 mg, 46  $\mu\text{mol}$ ; 63%).  $^1\text{H}$  NMR (300 MHz,  $\text{CD}_3\text{OD}$ ):  $\delta$  = 1.56 (s, 9H; *t*-Bu), 2.9–4.4 (m, 90H; ether), 7.19 (t,  $J$  = 6.5 Hz, 1H; 6-Py), 7.39 (s, 4H; Ph), 7.68 (t,  $J$  = 7.0 Hz, 1H; 4-Py), 7.77 (d,  $J$  = 8.3 Hz, 2H; Ph), 7.84 (d,  $J$  = 7.7 Hz, 1H; 5-Py), 8.00 (d,  $J$  = 8.3 Hz, 2H; Ph), 8.11 (d,  $J$  = 4.2 Hz; 3-Py), 8.79 (s, 4H; pyrrole- $\beta$ ), 8.90 (d,  $J$  = 4.5 Hz, 2H; pyrrole- $\beta$ ), 9.55 ppm (d,  $J$  = 4.5 Hz, 2H; pyrrole- $\beta$ ).  $^{13}\text{C}$  NMR (75 MHz,  $\text{CDCl}_3$ ):  $\delta$  = 28.54, 58.39, 59.11, 69.36, 69.92, 70.08, 70.57, 70.66, 70.75, 70.81, 70.90, 71.14, 72.06, 72.85, 80.89, 93.88, 97.89, 115.68, 116.66, 121.75, 122.34, 122.99, 127.53, 131.13, 131.74, 132.20, 132.86, 135.02, 136.34, 137.56, 138.14, 138.21, 143.82, 149.61, 149.82, 150.09, 150.68, 152.79, 153.12 ppm (Figure S6). MALDI-TOF MS (dithranol):  $m/z$ : calcd for  $\text{C}_{92}\text{H}_{120}\text{N}_6\text{O}_{26}\text{Zn}$ : 1788.75; found: 1788.83.  $\lambda_{\text{max}}$  in  $\text{CHCl}_3$ : 441, 509, 618 nm.

**4.2.5. 5-Bromo-15-(4-methoxyphenylethynyl)-10,20-bis[3,4,5-tris(9-methoxy-1,4,7-trioxanonyl)phenyl]porphyrinatozinc(II) (4).** Porphyrin **4** was synthesized by the Mizoroki–Heck type cross-coupling procedure, essentially same with that for the synthesis of porphyrin **3**. The deoxygenated mixture of porphyrin **2** (0.43 g, 0.26 mmol) and 4-ethynylanisole<sup>20</sup> (36 mg, 0.27 mmol) in THF (15 mL) and triethylamine (2.1 mL) was added triphenylarsine (46 mg, 0.15 mmol) and  $\text{Pd}_2(\text{dba})_3$  (22 mg, 24  $\mu\text{mol}$ ) stirred at 50 °C in the dark for 5 h. The crude mixture was washed with brine and the organic layer was dehydrated by anhydrous sodium sulfate. The chromatographic separation with chloroform–ethyl acetate–methanol (90/7/3, v/v/v) furnished the target porphyrin **4** and 5,15-bis(4-methoxyphenylethynyl)-10,20-bis[3,4,5-tris(9-methoxy-1,4,7-trioxanonyl)phenyl]porphyrinatozinc(II) as the byproduct. These porphyrins were difficult to be completely separated by silica-gel column at this stage and used for the next step without further purification. MALDI-TOF MS (dithranol):  $m/z$ : calcd for  $\text{C}_{83}\text{H}_{109}\text{BrN}_4\text{O}_{25}\text{Zn}$ : 1704.59; found: 1704.24.

**4.2.6. 5-{*N*-(*tert*-butoxycarbonyl)-4-anilino}-15-(4-methoxyphenylethynyl)-10,20-bis[3,4,5-tris(9-methoxy-1,4,7-trioxanonyl)phenyl]porphyrinatozinc(II), Zn(ArPor).** Zn(ArPor) was

prepared by the Suzuki–Miyaura cross-coupling procedure, essentially same with that for Zn(PyPor). The mixture of porphyrin **4** (0.21 g, 0.074 mmol) and pinacol 4- $\{N$ -(*tert*-butyloxycarbonyl)aminophenyl}boronate (57 mg, 0.18 mmol) in DMF (10 mL) and toluene (20 mL) was degassed by the Schlenk technique. The mixture was added caesium carbonate (50 mg, 0.15 mmol) and Pd(PPh<sub>3</sub>)<sub>4</sub> (19 mg, 0.015 mmol), and then allowed for stirring at 80 °C in the dark for 5 h. The reaction mixture was passed through a Celite pad and the solvent was removed under reduced pressure. The crude material redissolved in dichloromethane was washed with water and brine. The organic layer separated was dried over anhydrous sodium sulfate. The titled material was roughly purified by silica-gel column chromatography with chloroform–ethyl acetate–methanol (90/7/3, v/v/v). Further purification was subjected to recycling GPC with chloroform as the eluent. Zn(ArPor) was obtained as a viscous green substance (29 mg, 0.016 mmol; 6% through 2 steps from **2**). <sup>1</sup>H NMR (300 MHz, CD<sub>3</sub>OD):  $\delta$  = 1.59 (s, 9H; *t*-Bu), 3.06–3.85 (m, 78H; ether), 3.73 (s, 3H; methoxy), 4.15 (m, 12H; Ph-OCH<sub>2</sub>-), 6.90 (d,  $J$  = 8.7 Hz, 2H; Ph), 7.48 (s, 4H; Ph), 7.75 (d,  $J$  = 2.9 Hz, 2H; Ph), 7.78 (d,  $J$  = 3.0 Hz, 2H; Ph), 8.02 (d,  $J$  = 8.5 Hz, 2H; Ph), 8.79 (d,  $J$  = 4.7 Hz, 2H; pyrrole- $\beta$ ), 8.83 (d,  $J$  = 4.7, 2H; pyrrole- $\beta$ ), 8.98 (d,  $J$  = 4.6 Hz, 2H; pyrrole- $\beta$ ), 9.71 ppm (d,  $J$  = 4.6 Hz, 2H; pyrrole- $\beta$ ) (Figure S9). <sup>13</sup>C NMR (75 MHz, CDCl<sub>3</sub>):  $\delta$  = 28.47, 55.48, 58.17, 59.07, 69.39, 69.71, 70.10, 70.51, 70.62, 70.70, 70.76, 70.86, 72.02, 72.76, 77.22, 77.44, 114.40, 115.70, 116.56, 133.07, 138.16, 150.64, 152.15 ppm. MALDI-TOF MS (dithranol):  $m/z$ : calcd for C<sub>94</sub>H<sub>123</sub>N<sub>3</sub>O<sub>27</sub>Zn: 1817.77; found: 1817.37.  $\lambda_{\text{max}}$  in CHCl<sub>3</sub>: 445, 573, 622 nm.

**4.2.7. Pinacol 4- $\{N$ -(*tert*-butyloxycarbonyl)aminophenyl} boronate.** Borylation of *tert*-butyl 4-iodophenylcarbamate<sup>21</sup> was carried out according to literature procedures.<sup>22</sup> A solution of *tert*-butyl 4-iodophenylcarbamate (0.36 mg, 1.1 mmol) in 1,4-dioxane (10 mL) and triethylamine (0.5 mL) was degassed *via* freeze-pump-thaw cycles and flushed with argon gas in a Schlenk flask. To the solution was added pinacol borane (1.45 mL, 10 mmol) and PdCl<sub>2</sub>(dppf) (dppf = 1,1'-bis(diphenylphosphino)ferrocene) (39 mg, 47  $\mu$ mol). The mixture was gently refluxed at 100 °C for 2 h. The reaction mixture diluted with dichloromethane was washed with water and brine. The organic layer separated was dried over anhydrous sodium sulfate. Recrystallization from methanol gave the target material as colorless needle crystal (0.16 g, 0.45 mmol; 45%). <sup>1</sup>H NMR (300 MHz, CD<sub>3</sub>OD):  $\delta$  = 1.33 (s, 12H, Me), 1.52 (s, 9H; *t*-Bu), 7.36 (d,  $J$  = 8.5 Hz, 2H; Ph), 7.73 ppm (d,  $J$  = 8.5 Hz, 2H; Ph).

### 4.3. Preparation of aqueous self-assemblies

The porphyrins were dissolved in methanol, prior to dissolution in water. Then, 5.0  $\mu$ L of the methanol solution (*ca.* 1.2 mM of Zn(PyPor) or Zn(ArPor)) was injected into 3.0 mL of distilled water and adjusted to *ca.*  $2 \times 10^{-6}$  M of concentration in water. The solution was allowed to stand for a few days.

The Soret band emerged around 420 nm immediately after dissolution of Zn(PyPor) in water. That gradually shifted to around 470 nm over a few hours. In this period, fluorescence intensity was very weak with remaining similar level. After aging for a few days, spectral evolution of the Soret band was converged

from 420 nm to the stationary band at 463 nm, with remarkable increment of fluorescent emission.

The properties of the porphyrin assemblies examined were much affected by several experimental parameters. For example, the content of methanol used for initial dissolution significantly influenced the reproducibility of the spectral properties. When the content of methanol was increased, the aqueous self-assemblies were loosened to lose the susceptibility to the external ligand. Also, spectral behaviour varied depending on ionic strength and temperature. At higher temperature than 30 °C, bolaamphiphilic porphyrin was precipitated, probably due to dehydration of oligo-ether side-chains.<sup>23</sup> On the other hand, the porphyrin assemblies were too robust to be coordinated by the external ligand binding at lower temperature than 15 °C. When the aqueous media was buffered with Na<sub>2</sub>HPO<sub>4</sub>–NaH<sub>2</sub>PO<sub>4</sub>, the solubility of bolaamphiphilic porphyrin was seriously reduced. Then, the present experiments were performed in distilled water (*~*pH 6.8) at 25 °C.

In the main text, the dissociation behaviors were described unless the amphiphilic assemblies collapsed. When the assemblies were collapsed, the spectral change showed discontinuous in the titration experiments. The collapse behaviours were coincidentally observed epifluorescence microscopy. Addition of excess amount of pyridyl ligand dissolved the amphiphilic assemblies into apparently isotropic solution.

### Acknowledgements

The authors are grateful to Prof. S. Asaoka and Dr S. Masuo (Kyoto Institute of Technology) for GPC purification and epifluorescence microscopic observation, respectively. This work was partly aided by financial supports from JST (Japan Science and Technology Agency) Innovation Plaza Kyoto, through a Grant-in-Aid for Young Scientists (B) (No. 21750123) from JSPS (Japan Society of the Promotion of Science), and the Kyoto-Advanced Nanotechnology Network program with technical assistance by Ms. Y. Nishikawa (Nara Institute of Science and Technology).

### Notes and references

- (a) A. Satake and Y. Kobuke, *Tetrahedron*, 2005, **61**, 13–41; (b) I. Beletskaya, V. S. Tyurin, A. Y. Tsivadze, R. Guillard and C. Stern, *Chem. Rev.*, 2009, **109**, 1659–1713, and cited therein.
- (a) K. A. Connors, *Binding Constant, The Measurement of Molecular Complex Stability*, John Wiley & Sons, 1987; (b) C. A. Hunter and H. L. Anderson, *Angew. Chem., Int. Ed.*, 2009, **48**, 7488–7499.
- (a) K. M. Smith, L. A. Kehres and J. Fajer, *J. Am. Chem. Soc.*, 1983, **105**, 1387–1389; (b) A. Jesorka, T. S. Balaban, A. R. Holzwarth and K. Schaffner, *Angew. Chem., Int. Ed. Engl.*, 1996, **35**, 2861–2863.
- (a) R. T. Stibrany, J. Vasudevan, S. Knapp, J. A. Potenza, T. Emge and H. J. Schugar, *J. Am. Chem. Soc.*, 1996, **118**, 3980–3981; (b) N. N. Gerasimchuk, A. A. Mokhir and K. R. Rodgers, *Inorg. Chem.*, 1998, **37**, 5641–56650.
- M. Koepf, J. A. Wytko, J.-P. Bucher and J. Weiss, *J. Am. Chem. Soc.*, 2008, **130**, 9994–10001.
- (a) Y. Kobuke and H. Miyaji, *J. Am. Chem. Soc.*, 1994, **116**, 4111–4112; (b) K. Kameyama, M. Morisue, A. Satake and Y. Kobuke, *Angew. Chem., Int. Ed.*, 2005, **44**, 4763–4766; (c) M. Morisue and Y. Kobuke, *Chem.–Eur. J.*, 2008, **14**, 4993–5000.
- (a) J. Ribó, J. Crusats, F. Sagüés, J. Claret and R. Rubires, *Science*, 2001, **292**, 2063–2066; (b) C. Escudero, J. Crusats, I. Diez-Pérez, Z. El-Hachemi and J. M. Ribó, *Angew. Chem., Int. Ed.*, 2006, **45**, 8032–8035.

- 8 (a) M. Y. Choi, J. A. Pollard, M. A. Webb and J. L. McHale, *J. Am. Chem. Soc.*, 2003, **125**, 810–820; (b) S. Okada and H. Segawa, *J. Am. Chem. Soc.*, 2003, **125**, 2792–2796.
- 9 (a) G. McDermott, S. M. Prince, A. A. Freer, A. M. Hawthornthwaite-Lawless, M. Z. Papiz, R. J. Cogdell and N. W. Isaacs, *Nature*, 1995, **374**, 517–521; (b) A. W. Roszak, T. D. Howard, J. Southall, A. T. Gardiner, C. J. Law, N. W. Isaacs and R. J. Cogdell, *Science*, 2003, **302**, 1969–1972.
- 10 (a) G. Steinberg-Yfrach, J.-L. Rigaud, E. N. Durantini, A. L. Moore, D. Gust and T. A. Moore, *Nature*, 1998, **392**, 479–482; (b) T. Komatsu, M. Moritake and E. Tsuchida, *Chem.–Eur. J.*, 2003, **9**, 4626–4633; (c) N. Nagata, Y. Kuramochi and Y. Kobuke, *J. Am. Chem. Soc.*, 2009, **131**, 10–11.
- 11 (a) T. Kunitake, *Angew. Chem., Int. Ed. Engl.*, 1992, **31**, 709–726; (b) J.-H. Fuhrhop and T. Wang, *Chem. Rev.*, 2004, **104**, 2901–2937; (c) J.-H. Ryu, D.-J. Hong and M. Lee, *Chem. Commun.*, 2008, 1043–1054.
- 12 M. Kasha, *Radiat. Res.*, 1963, **20**, 55–71.
- 13 T. Yamaguchi, T. Kimura, H. Matsuda and T. Aida, *Angew. Chem., Int. Ed.*, 2004, **43**, 6350–6355.
- 14 H. Nakamura, H. Fujii, H. Sakaguchi, T. Matsuo, N. Nakashima, K. Yoshihara, T. Ikeda and S. Tazuke, *J. Phys. Chem.*, 1988, **92**, 6151–6156.
- 15 The binding constant of axial ligand in chloroform: pyridine;  $2.9 \times 10^3 \text{ M}^{-1}$  for Zn(PyPor), and  $1.8 \times 10^3 \text{ M}^{-1}$  for Zn(ArPor). Axial coordination was substantially not observed for 2,6-lutidine.
- 16 The log*P* value: 0.65 for pyridine and 1.68 for 2,6-lutidine.
- 17 (a) T. Mizutani, K. Wada and S. Kitagawa, *J. Am. Chem. Soc.*, 1999, **121**, 11425–11431; (b) R. Murakami, A. Minami and T. Mizutani, *Org. Biomol. Chem.*, 2009, **7**, 1437–1444; (c) S. Tomas and L. Milanesi, *J. Am. Chem. Soc.*, 2009, **131**, 6618–6623.
- 18 T. Sakurai, K. Shi, H. Sato, K. Tashiro, A. Osuka, A. Saeki, S. Seki, S. Tagawa, S. Sasaki, H. Masunaga, K. Osaka, M. Tanaka and T. Aida, *J. Am. Chem. Soc.*, 2008, **130**, 13812–13813.
- 19 S. Takahashi, Y. Kuroyama, K. Sonogashira and N. Hagihara, *Synthesis*, 1980, 627–629.
- 20 L. F. Tietze, C. A. Vock, I. K. Krimmelbein, J. M. Wiegand, L. Nacke, T. Ramachandar, K. M. D. Islam and C. Ga, *Chem.–Eur. J.*, 2008, **14**, 3670–3679.
- 21 A. Yokoyama, T. Maruyama, K. Tagami, H. Masu, K. Katagiri, I. Azumaya and T. Yokozawa, *Org. Lett.*, 2008, **10**, 3207–3210.
- 22 O. Baudoin, D. Guénard and F. Guéritte, *J. Org. Chem.*, 2000, **65**, 9268–9271.
- 23 W. Li, A. Zhang and A. D. Schlüter, *Chem. Commun.*, 2008, 5523–5525.